Title

MOLECULAR THERMODYNAMICS OF AQUEOUS SOLUTIONS CONTAINING ELECTROLYTES AND NONELECTROLYTES

Authors

Kruppa, R.K.
Harvey, A.H.
Prausnitz, J.M.

Publication Date

1987-10-01

LBL-24206
Preprint

Lawrence Berkeley Laboratory
UNIVERSITY OF CALIFORNIA

Materials & Chemical Sciences Division

Submitted for publication

Molecular Thermodynamics of Aqueous Solutions Containing Electrolytes and Nonelectrolytes

R.K. Kruppa, A.H. Harvey, and J.M. Prausnitz

October 1987

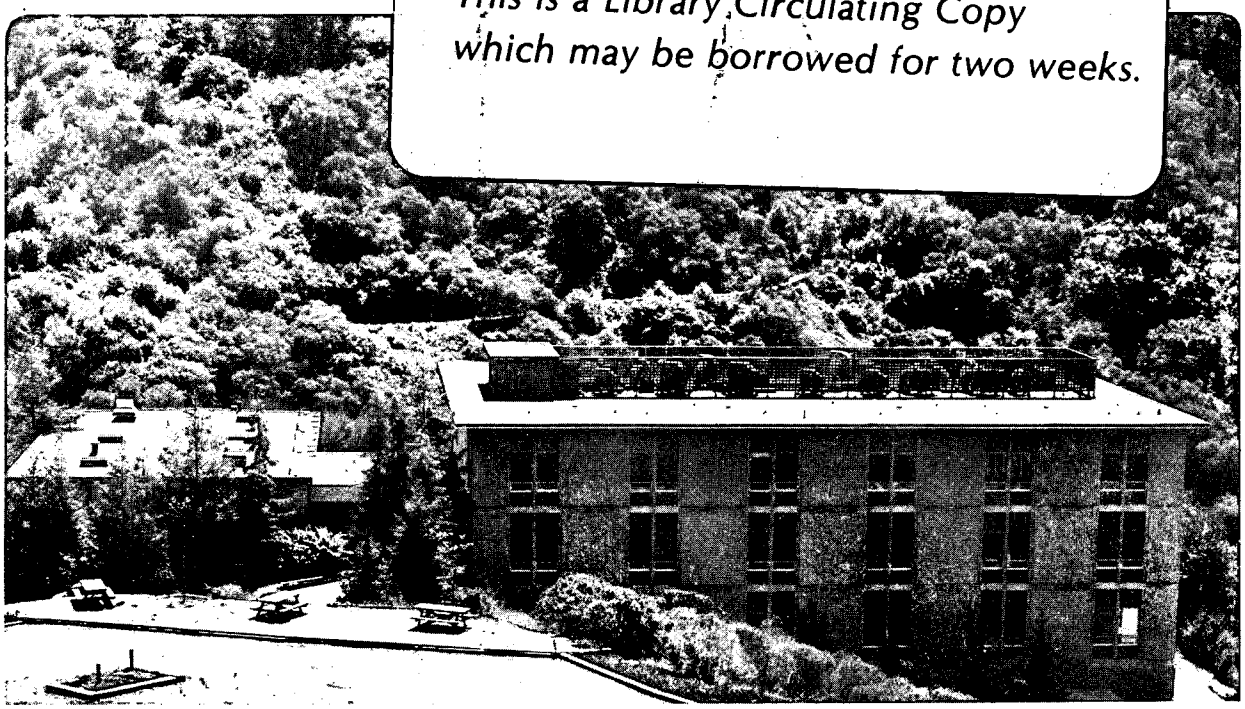

Prepared for the U.S. Department of Energy under Contract DE-AC03-76SF00098

DISCLAIMER

Molecular Thermodynamics of Aqueous Solutions Containing Electrolytes and Nonelectrolytes

Robert K. Kruppa
Allan H. Harvey
and
John M. Prausnitz

Materials and Chemical Sciences Division
Lawrence Berkeley Laboratory
and
Chemical Engineering Department
University of California
Berkeley, California 94720

This work was supported by the Director, Office of Energy Research, Office of Basic Energy Sciences, Chemical Sciences Division of the U.S. Department of Energy under Contract No. DE-AC03-76SF00098.

Table of Contents

Abstract

To measure phase equilibrium data in mixtures containing electrolytes and nonelectrolytes, an experimental apparatus is designed and constructed. The composition of both phases is analyzed from small samples. A circulation system mixes the components to ensure equilibrium. The equipment can withstand conditions of 250 °C and 140 MPa. Experimental safety is a key element of the design. It can be used for systems containing combustible gases; the first application is to measure the solubility of CH_4 in NaCl solutions at high pressures.

Phase equilibria are predicted from a new equation of state applicable to high pressures and all practical fluid densities. The Helmholtz energy of a mixture of electrolytes and nonelectrolytes is calculated from molecular theory. Pure-component and binary parameters are used to adjust the equation of state to experimental data. The model predicts the solubility of CO_2 in pure water at pressures up to 100 MPa with a maximum deviation of less than 0.3 mole percent. When applied to ternary mixtures containing electrolytes, the salting-out effect is represented correctly even at high pressures.

1. Introduction

Molecular thermodynamics emphasizes the powerful combination of theoretical tools and experimental findings. While phase equilibria are elegantly described by classical thermodynamics, application of theory to practice is not straightforward. Abstract thermodynamic quantities must be related to physical phenomena.

The macroscopic properties of substances (for example, density or vapor pressure) are determined by interactions on a microscopic level. Molecular theory interprets and correlates the forces between elementary particles and relates them to thermodynamic variables such as energy and entropy. Reliable experimental data are essential for such interpretation and correlation. Thermodynamic models for phase equilibria must be critically evaluated and adjusted on the basis of experimental facts.

Phase equilibria in systems containing aqueous electrolytes and nonelectrolytes at high pressures are of interest in several areas. Economically significant quantities of natural gas are dissolved in geopressured brine reservoirs, called aquifers. Precise knowledge of the phase equilibria in such systems will be important to the use of aquifers as an energy resource. In addition, the formation of crystals in geothermal brines is largely governed by the solubility of both electrolytes and nonelectrolytes in aqueous phases, often at high temperatures and pressures. New insight into such systems will help the understanding of geochemical processes.

Progress in this field must be made in two aspects. Experimental data for the solubility of gases in salt solutions is still relatively scarce, especially at extreme conditions of temperature and pressure. Furthermore, better thermodynamic models must be developed to predict phase equilibria in such systems over a wide range of conditions. Both the experimental and the theoretical side are addressed in this work.

Chapter 2 describes design and construction of an experimental apparatus to investigate fluid-phase equilibria at high pressures. Designed for aqueous mixtures containing salt and volatile nonelectrolytes, this apparatus is intended to provide data for the compositions of both the liquid and the vapor phase.

The engineering application of molecular thermodynamics follows from its ability to predict phase equilibria, using a minimum of experimental information. Based on molecular theory, we developed a model for systems containing both electrolytes and nonelectrolytes. Chapter 3 describes our model, which uses an equation of state applicable to vapor and liquid phases and which may include supercritical components.

2. An Experimental Apparatus for Measuring High-Pressure Vapor-Liquid Equilibria in Systems Containing Aqueous Electrolytes

2.1. Introduction

Experimental data are essential to understanding nature's behavior. Suitable models to describe natural phenomena must be based on reliable measurements. For equilibrium thermodynamics, we require an accurate description of the behavior of pure substances as well as mixtures.

The equipment developed in this work is useful for measuring vapor-liquid equilibria in systems with three components: water, salt, and a volatile nonelectrolyte. The first application is for the mixture H_2O, NaCl, and CH_4.

The thermodynamic state of a stable ternary fluid phase can be described by five independent variables; pressure P, temperature T, molar volume v, and two compositions z_i. The concentration of the third component follows from the requirement that the sum of the individual mole (or weight) fractions add up to unity. In general, two different methods are available to collect vapor-liquid equilibrium data:

1. Following the synthetic procedure, carefully measured amounts of each component are injected into a vessel of determined size, providing a mixture of known molar volume and global composition. Starting with the sample present in a homogeneous state, temperature and pressure in the experimental vessel are varied until a phase transition occurs. This transition may be detected by direct observation or by tracking a suitable property, such as the electrical conductivity. Temperature and pressure at this point are registered. Together with the known molar volume and composition of the sample, they provide a single point on the phase envelope. Using an experimental cell of variable volume, such as a cylinder with matching piston, several isochores of the system can be measured with just one synthetic mixture. However, except for the binary case, no information about the individual compositions of the corresponding phases is available. Systems of three or more components possess more internal degrees of freedom than can be controlled in this type of experiment.

2. In the analytic method, two phases are allowed to equilibrate in a suitable vessel at constant temperature and pressure. Small samples are drawn from both phases and analyzed for composition, often by chromatographic methods. These analyses provide one point for each ternary phase in the (P, T, z_1, z_2) phase diagram. Data for the individual molar volumes are more difficult to obtain by this procedure. The global composition of the mixture originally introduced into the vessel must be known. The position of the phase boundary must be measured to indicate the volume of each phase. In addition, a suitable expression is required for the partial molar volumes of the components in one of the phases.

To develop an equation of state which describes vapor-liquid equilibrium, we require precise data for the compositions of both phases. Accordingly, the apparatus developed and constructed in this work uses the analytic method. Phase equilibrium is reached in a high-pressure autoclave; a circulation system allows for sufficient mixing of the components. Separate samples can be drawn from both phases and analyzed for composition in a gas chromatograph. No attempt is made to measure liquid or vapor phase densities. The equipment is designed for temperatures from ambient to 250°C and pressures to 140 MPa.

2.2. Equilibrium Cell and Circulation System

The equipment necessary to maintain the phase equilibrium is contained in a main oven which is a constant-temperature bath of nitrogen gas. It is shown in Figure 2-1.

The central component is a high-pressure vessel of approximately 100 cm^3 internal volume, designed and manufactured by Autoclave Engineers of Erie, Pennsylvania. Because of the high pressure and the presence of chloride ions, the material used is annealed, age-hardened K-Monel 500, a corrosion-resistant nickel alloy of high strength. The cell consists of a cylindrical body with 3.25-inch (82.6-mm) external diameter and 1.25-inch (31.8-mm) bore.

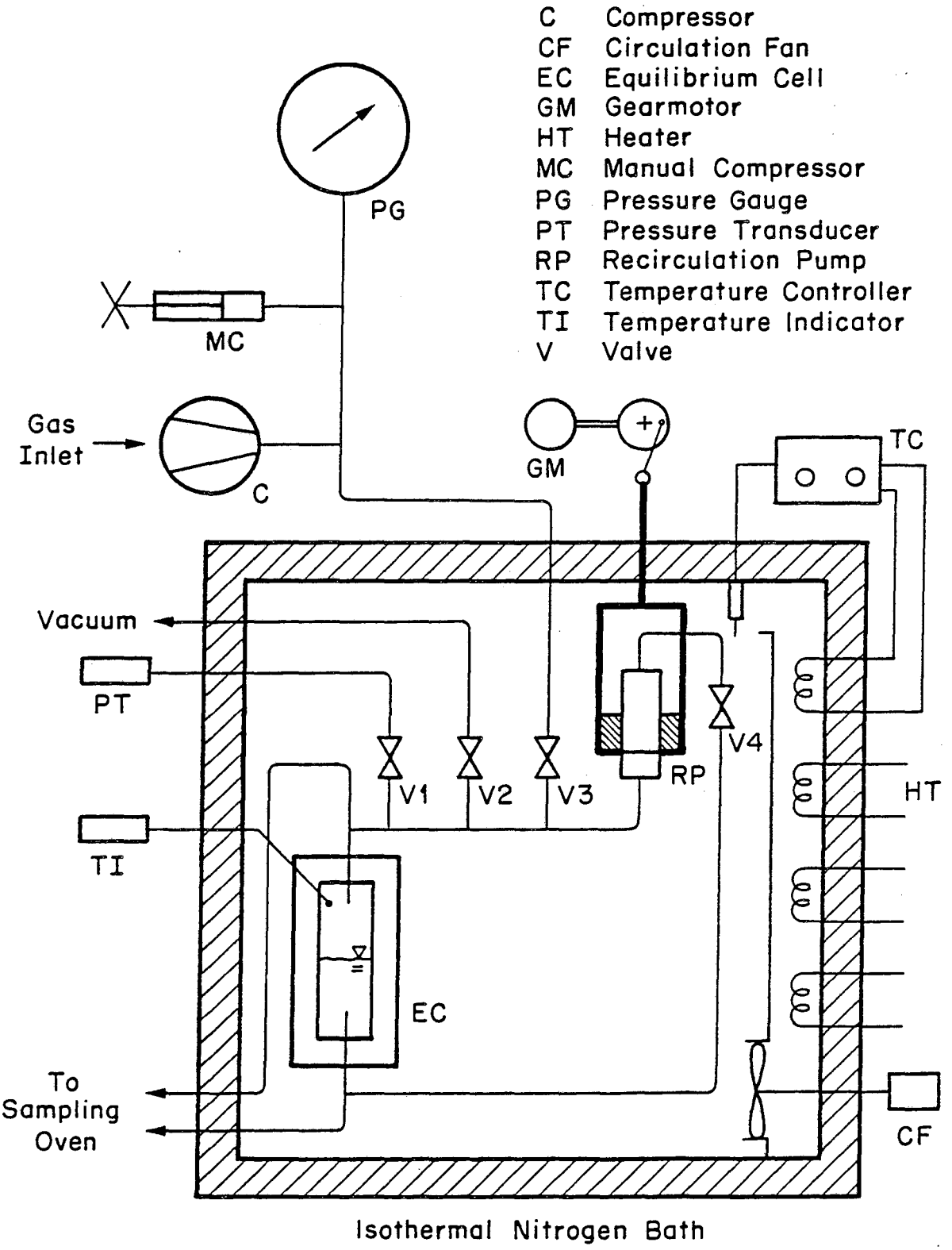

Figure 2-1: Main Oven with Equilibrium Cell

A self-sealing closure (Autoclave Engineers) forms its top end. The internal pressure forces a cover body into a conical seal ring and presses it against the outside cylinder. Both the cover and the ring are also made of K-Monel.

By the use of slightly different angles between the surfaces of the cover, seal ring, and body, line contact results to form the seal. Both ends of the autoclave have appropriate connections for high-pressure tubing.

The liquid and vapor phases occupy approximately equal portions of the vessel volume. To ensure that material equilibrium between the two is reached shortly after the temperature and pressure of the cell have been adjusted, the mixture must be agitated. The thick walls of the autoclave and the corrosive nature of the salt solution make the use of a magnetic stirrer impossible. Instead, we include a circulation line with a piston pump. Some of the vapor phase is drawn off the vessel's top and pumped back into the bottom, where it bubbles through the liquid, providing good mass transfer between the phases and reducing the time necessary to reach equilibrium. Before sampling, the circulation must be turned off for several minutes to allow the system to settle.

A schematic diagram of the piston pump is shown in Figure 2-2. It is specifically designed for this apparatus, although similar instruments have been used elsewhere.[1] The body is again made of K-Monel 500, which is paramagnetic. It is sealed by a metal-to-metal conical closure. The inner bore of the pump is honed to a diameter of 0.375-inch (9.5-mm). A piston made of solid nickel fits into the cylinder with a very close tolerance. No O-rings of elastomeric materials could be used to seal between the two because of the high temperatures and because methane gas might cause swelling.

Nickel is ferromagnetic and attracted to the field of a ring magnet placed outside the pump body. Moving the magnet up and down causes the pumping action; two ball-type check valves ensure that flow occurs only in the upward direction. The lower valve closes upon the downstroke while the other opens, thus transferring the gas from below to above the piston. The situation reverses on the upstroke, forcing the gas around the circulation line and simultaneously filling the lower pump chamber with a new charge.

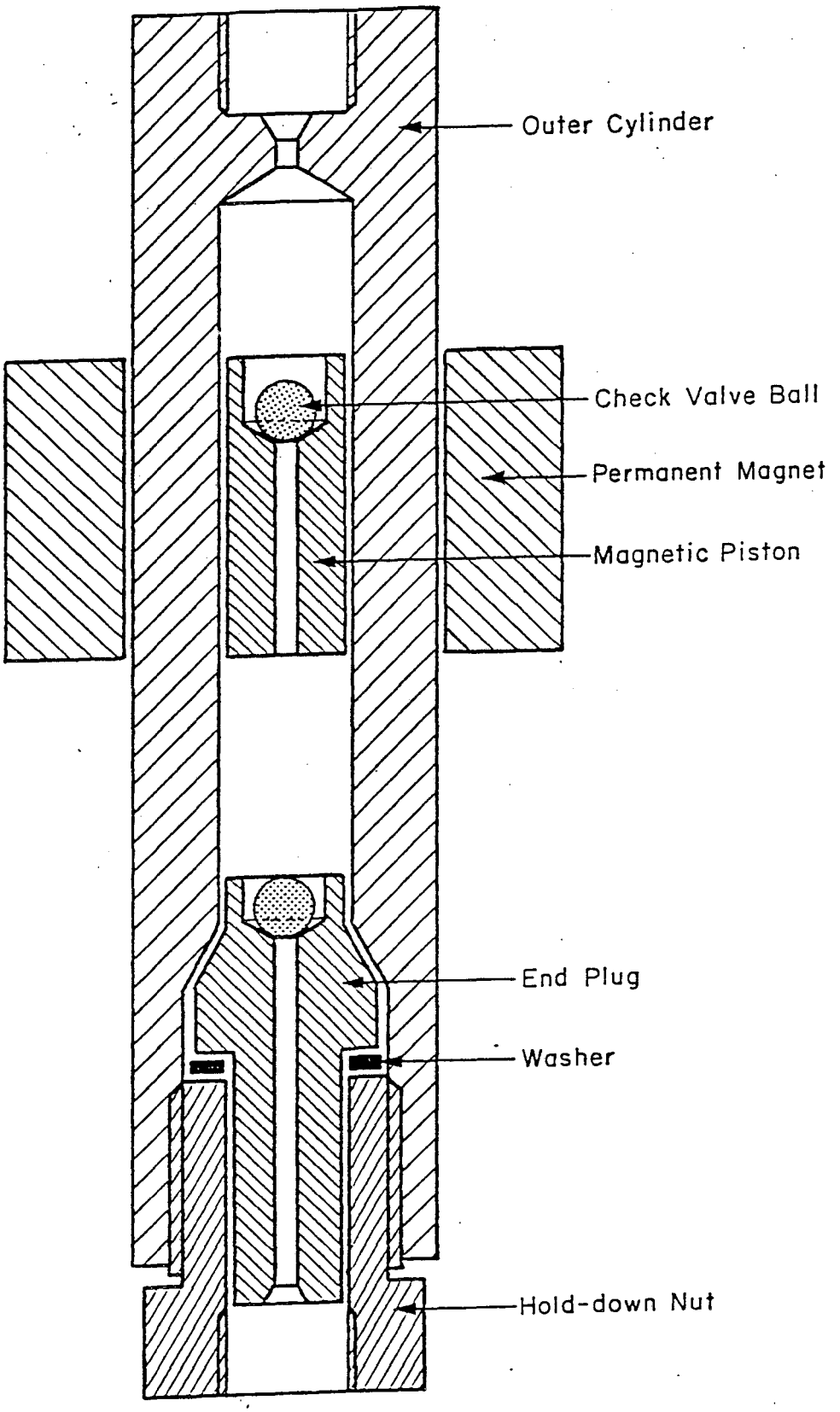

Figure 2-2: Magnetic Circulation Pump

A piston rod connects the permanent magnet to the driving assembly located above the equilibrium oven. It is powered by a gearmotor with variable speed turning an eccentric disc. Both the frequency and the amplitude of the piston's motion can be adjusted to give optimum performance. Typical pump rates range from 30 to 60 strokes per minute.

All the high-pressure lines in the experiment are 1/4-inch tubing with an internal diameter of 0.083 inch (2.1 mm), the connections are metal-to metal and of the cone type. The lines which may come in contact with chloride ions, such as the circulation path, are made of Monel. Stainless steel is used for the remaining parts.

Several additional connections are necessary. A two-stage air-driven compressor pumps pure methane into the system; the pressure can be finely adjusted with a cylinder of variable volume, attached to the same line. To empty the cell between experiments, a vacuum pump is connected via a suitable valve. Not shown in Figure 2-1 is the line to charge the vessel with an initial salt solution and to drain the liquid after a run. The gas can be released to the open atmosphere outside the building through a vent valve and suitable exhaust pipe.

2.3. Sampling and Analysis

To analyze for the compositions using a gas chromatograph, small volumes must be drawn from the phases at equilibrium, preferably directly from the autoclave. For this purpose, thin capillary lines extend into both ends of the pressure cell. Running inside the high-pressure tubing, these lines end at appropriate sampling valves. Here, the inner and the outer tube are hard-soldered together, forming a tight seal. During sampling, flow occurs only through the capillary line whereas the external thick wall carries the stresses from the high pressure. Figure 2-3 shows a cross section of the assembly. This design has several advantages. There is no pressure difference across the walls of the sampling lines, allowing for very fine tubing.

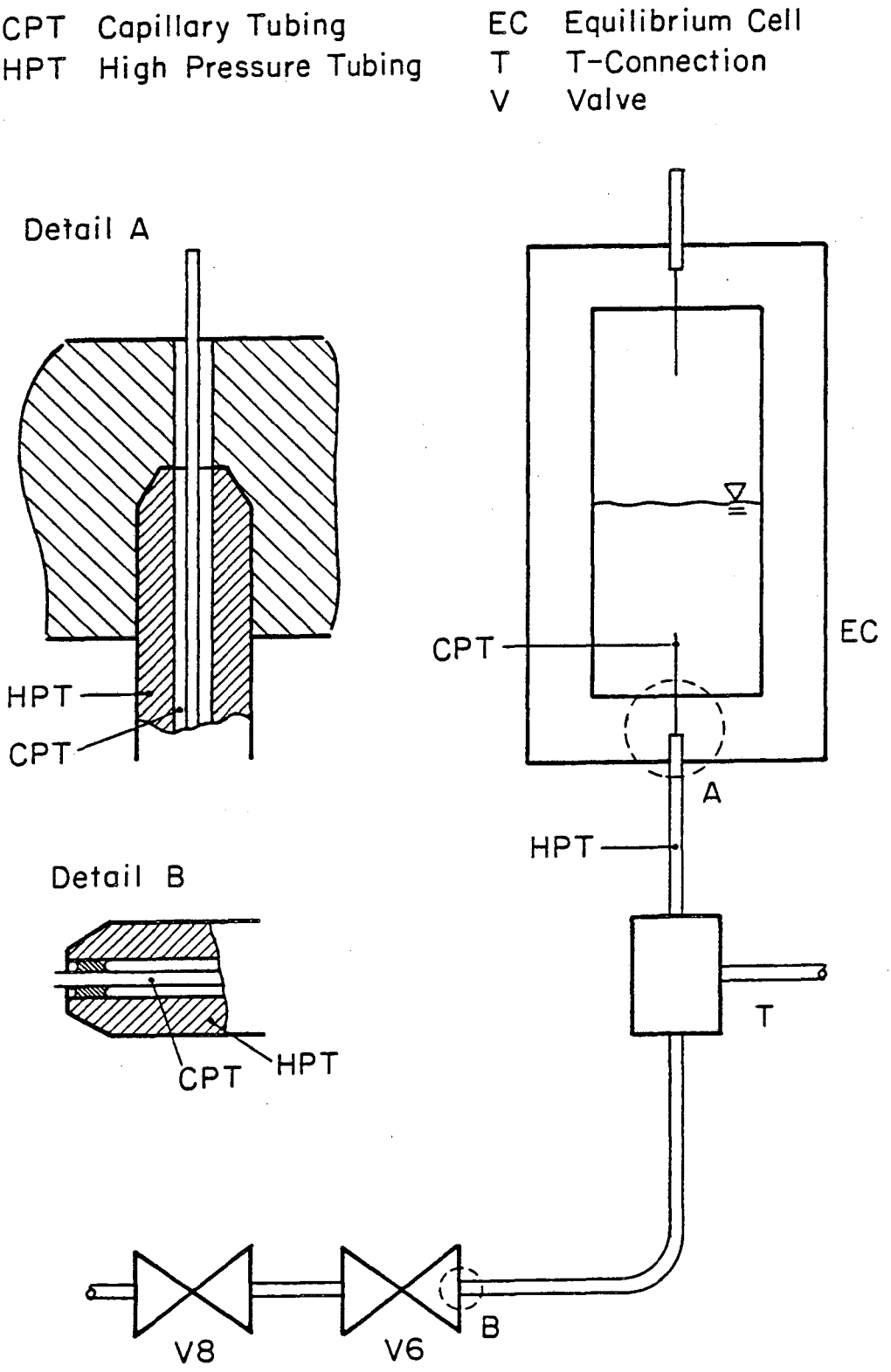

Figure 2-3: Sampling Line Assembly

We use capillaries with an internal diameter of 0.012 inch (0.3 mm), manufactured from corrosion-resistant Inconel alloy 600. Only a very small volume (approximately 0.1 cm^3 for the longer of the two lines) must be purged before obtaining the equilibrium phase from the autoclave. As a result, upon sampling, the pressure drop in the cell is kept to a minimum, leaving equilibrium conditions nearly unaltered.

The capillary runs through a tee coupling which joins the high-pressure lines of the circulation and from the sampling valve. Thus, both lines share one connection at each end of the autoclave.

A second nitrogen bath keeps the lines and valves necessary for sampling at a suitable temperature. This oven is shown in Figure 2-4. V5 and V6 are the primary sampling valves for the vapor and liquid phase, respectively. By opening one of these valves, the corresponding phase from the cell is allowed to fill the short piece of tubing to the secondary valve, V7 or V8. Closing the primary and opening the secondary valve expands the sample into the flash tank. The surrounding oven is kept at a temperature high enough to prevent condensation of water in the lines or the flash tank. The salt, virtually all of which is found in the liquid phase, crystallizes upon the expansion and does not reach the gas chromatograph. The solid salt has to be cleaned out regularly; the appropriate valves and lines are easily accessible.

Helium is used as the carrier gas for the analysis. It dilutes the sample and raises the pressure in the flash tank to 60 psi (0.4 MPa) as required by the gas chromatograph. Valve V11 connects the helium cylinder to the flash tank. By opening valve V9, some of the gaseous mixture is then allowed to fill the sample loop on a six-way valve. Turning the latter, this volume is injected into the carrier-gas stream to the chromatograph. The line from the sampling oven to the inlet port of the chromatograph is covered with electrical heating tape, preventing condensation of water in the tubing.

Essentially all of the salt is in the liquid phase. Its concentration only needs to be measured initially, when charging the cell with solution. Also, the percentage of the cell volume originally occupied by the liquid phase must be known. Then, using the known vapor pressure of water, allows us to adjust for the change in salinity at higher temperatures.

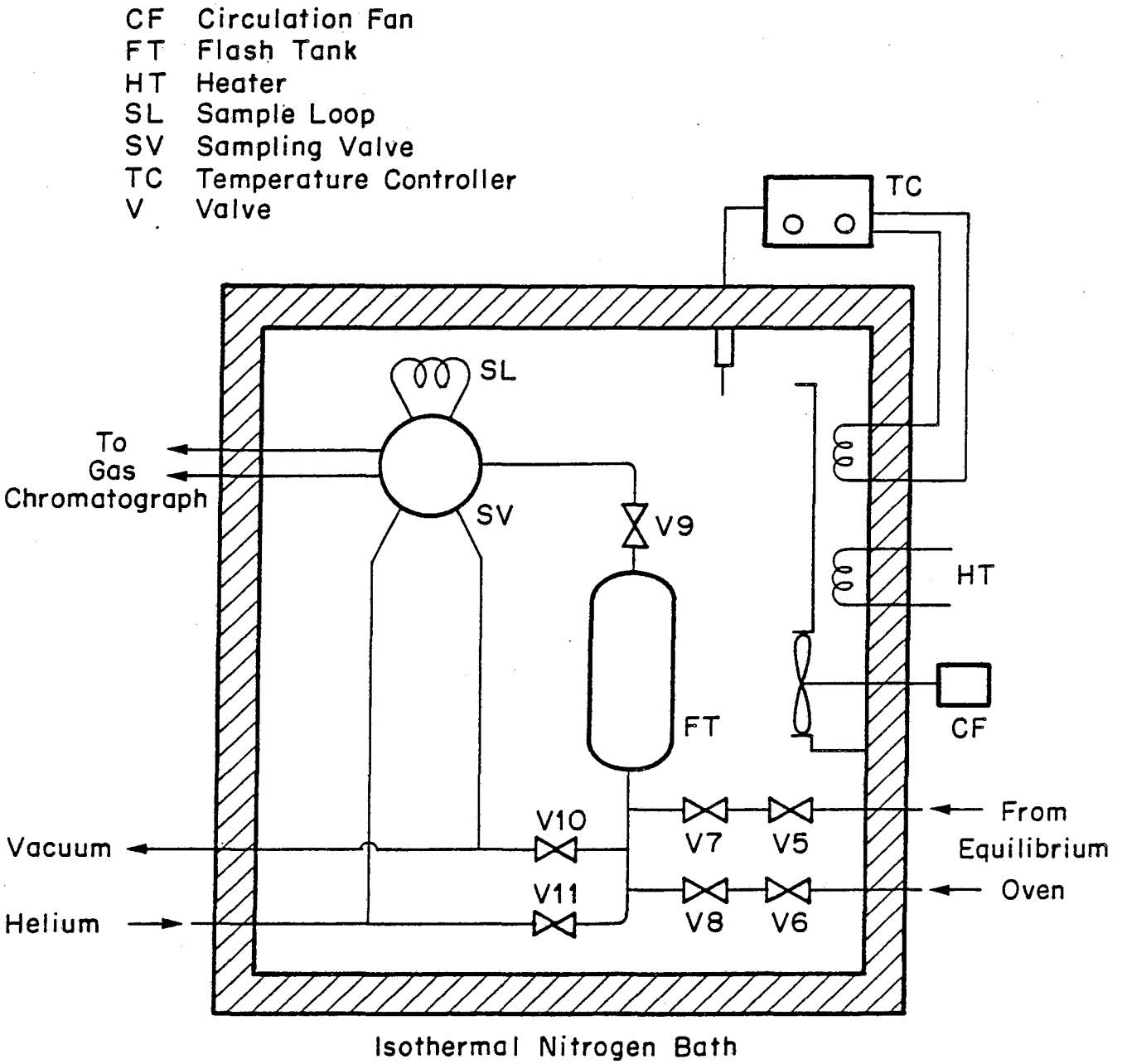

Figure 2-4: Sampling Oven

The pressure in the autoclave is monitored with a strain-gauge transducer connected to a digital readout. Its range extends up to 170 MPa with a maximum uncertainty of 0.5 MPa at the highest reading.

At several locations within the main oven, the temperature is measured using chromel-alumel thermocouples. to ensure that undesirable temperature gradients in the nitrogen bath are detected. The temperature at equilibrium is recorded by a thermocouple located in a small hole in the thick wall of the autoclave. The measurements have an accuracy of better than 1 percent over the range room temperature to 250°C.

2.4. Temperature Control

Both ovens employ the same principle to provide isothermal conditions. They are heated by electric resistance heaters, equipped with fins of sheet metal to provide for good heat transfer. A narrow duct with openings at either end surrounds the heaters. The gas inside the oven is drawn through this channel by suitable circulation fans, resulting in a forced-convection heating assembly. An additional fan in the larger, main oven helps to disperse the gas inside and to minimize temperature gradients.

For each oven, some of the heaters are permanently connected and can be adjusted by rheostats. The others are switched on and off by a temperature controller, which in turn uses the signal from a thermocouple to maintain isothermal conditions. The fraction of on-time of the controlled heaters can be influenced by adjusting the rheostats on the manual circuits to give optimum results.

2.5. Safety Measures

The experiment incorporates several factors which require special attention regarding safety. Most important are the very high pressures and the presence of methane, a combustible gas. Also, the elevated temperatures in the two ovens and the danger of corrosion need to be considered. Much of the effort in designing the equipment was directed towards safe control of these factors and towards the protection of workers and instruments.

All equipment intended to contain gases at high pressures must be initially pressure-tested using a liquid content. The autoclave, rated to a

maximum working pressure of 25000 psi (172 MPa) was hydrotested by the supplier. After assembly of all high-pressure components, a further test of the entire system is necessary. The volume is evacuated and subsequently filled with water. As the compressibility of water is very small, the hand-operated spindle compressor can be used for the test. A suitable maximum testing pressure is 1.3 times the highest value reached in the experiment. There must not be any leaks at this testing pressure. In addition, the diameters of the autoclave and the circulation pump are measured before, during, and after the test. After depressurization, the vessels must return to their original sizes, indicating that there was no permanent deformation.

All components are protected against overpressure by rupture discs. These are thin metallic plates carefully manufactured to burst at a pressure lower than the limit of the component they protect. They are mounted between the system on one side and atmospheric vent lines on the other side. These vents release the gas to the outside of the building.

The apparatus includes a total of five rupture discs. Two discs, rated for 24000 psi (165 MPa), protect the experimental cell and the line from the compressor, respectively. In addition, the lines leading from high-pressure to low-pressure sections are equipped with suitable rupture discs of lesser ratings. In case a valve is accidentally opened (such as the one connecting the vacuum pump to the circulation line), these discs prevent overloading the low-pressure components.

Two valves, leading to the exhaust pipes, allow venting of the high-pressure sections manually at all times during the experiment. The gas can be safely released after a run or in case of any difficulty.

Due to the presence of methane gas, there is danger of forming combustible mixtures when a leak occurs. To prevent this, both ovens are purged with nitrogen, forming a buffer between the methane and atmospheric oxygen. To detect a leak quickly, a combustible gas sensor is installed inside the main oven. It sounds an alarm if traces of methane gas are found in the nitrogen bath.

Overheating the ovens is prevented by two methods: The temperature controllers include circuit breakers that turn off all power should the temperature exceed a preset upper limit. In addition, only a portion of the heaters is

automatically switched. Even if a controller should fail while in the ON-position, the resulting steady-state temperature will not rise dramatically above the intended value.

As a protection against an unforeseen accident, the entire apparatus is contained inside a sturdy safety barricade. It consists of a large steel-frame box with three rigid walls and a thick door to allow walk-in access to the ovens. The roof is covered with heavy gauge steel mesh; the entire structure is bolted to the floor. All controls necessary to conduct the experiment are extended to outside the enclosure; including valve handles, switches for heating and the circulation pump, as well as the gas chromatograph.

2.6. Experimental Procedure

Before an experiment, all components of the equipment must be tested for leaks using nitrogen gas. Then the equilibrium cell and the circulation line are evacuated.

After a salt solution is prepared, it must be degassed in a special tank outside the main oven. Degassing is achieved by drawing vacuum or by stripping with methane gas. The solution is transferred into the autoclave through a charging line and valve by applying a small pressure of methane on the degassing tank. The volume transferred into the cell must be monitored to ensure that approximately half of the high-pressure system is filled with liquid. A small portion of the liquid is drawn back out of the cell through a drain valve and analyzed for its concentration using atomic absorption spectrophotometry. This analysis is necessary because some water evaporates when degassing the liquid, changing its salinity.

The system is now ready for pressurizing with methane. It is advantageous to use the air-driven compressor to fill only the line up to valve V3, then turn off the compressor and slowly release the gas into the equilibrium cell. This procedure avoids hard pumping strokes acting directly on sensitive parts of the system, such as the pressure transducer.

Water and methane can form solid hydrates at low temperatures and high pressures. Therefore, the system should be pressurized to approximately 7 MPa and then heated to its final temperature before raising the pressure to higher values.

At all times when charging gas into the system, the piston of the circulation pump should be in its bottom position and valve V4 above the pump should be closed. These precautions prevent the piston from being driven out of the field of the permanent ring magnet and into the top end of the cylinder. The inside surface of the cylinder could not be honed to the end of the bore so that the piston may be trapped when it travels too high.

The final pressure in the autoclave may be closely adjusted by using the manual compressor to force the last portion of gas into the system. Then valve V3 is closed and the circulation is turned on to mix the vapor and liquid phases. Typically, equilibrium should be reached in 30 minutes. Before sampling, the pump is turned off and the system is allowed to settle. Samples from both phases are drawn in sequence and in a similar fashion.

The volume inside the capillary lines is purged by briefly opening the corresponding primary sampling valves (V5 or V7). After the sampling lines and the flash tank have been evacuated by opening valve V11, a sample is allowed to fill the small volume between the primary and secondary valve (i.e. V5 and V7 for the vapor phase). The primary valves must be opened very carefully when drawing the sample to avoid a sudden pressure drop across the capillary lines. These valves are equipped with special regulating stems which offer good control over the flowrate.

The sample is expanded into the flash tank through the secondary valve and subsequently mixed and diluted with helium by opening valve V11. Through valve V9, a small portion of the mixture is allowed to enter the evacuated sample loop on the six-way valve. For analysis, we use a dual column gas chromatograph (Varian) with thermal conductivity detectors and Poropak Q column packing. Several samples from the flash tank should be examined in sequence to ensure reproducibility of the results.

After both equilibrium phases have been sampled and analyzed, the conditions in the cell are changed to the next desired setting. It is advantageous to measure the equilibrium along isotherms with increasing pressure. More methane is forced into the system from the compressor line. To reduce the equilibrium pressure, some of the vapor phase should be vented to the atmosphere instead of cranking back the hand-operated compressor. Water from the equilibrium vapor could condense if drawn into the cold section of the

pressurizing line outside the equilibrium oven.

When discharging the system after a run, the pressure has to be released before lowering the temperature to avoid formation of hydrates. After most of the gas is vented to the atmosphere, the liquid can be drained through the appropriate valve.

3. An Equation of State for Mixtures Containing Aqueous Electrolytes and Supercritical Gases

3.1. Introduction

The macroscopic thermodynamic properties of matter are determined by the interactions of molecules or ions. Molecular thermodynamics provides a method to model equilibrium phenomena in mixtures containing widely different components, such as aqueous solutions of electrolytes. The forces between elementary particles are calculated and averaged according to the principles of statistical mechanics. Classical thermodynamics, coupled with molecular physics, is used to determine macroscopic equilibrium properties.

This work presents an equation of state applicable to all fluid densities from the ideal-gas limit to liquid-like densities. The properties of both phases are calculated from the same equation of state.

The framework using an equation of state is essential for application to mixtures which contain both subcritical and supercritical components. Calculations over wide ranges of temperature and pressure are possible.

An equation of state is most conveniently constructed by expressing the Helmholtz energy of a particular system. After a brief review of the thermodynamic background, this chapter presents several contributions to the Helmholtz energy resulting from different molecular interactions. Two terms describe the nonionic forces in a fluid phase. Others, concerned with permanent charges of ions, give rise to two additional terms of Helmholtz energy.

The equation of state is applied to the system of H_2O, NaCl, and CO_2. Calculated results for the binary mixtures of H_2O / CO_2 and H_2O / NaCl are compared with experimental data. In a further step, the model is used to predict the solubility of CO_2 in aqueous NaCl solutions. Deviations between experimental data and calculated properties form the basis for a critical analysis of our model and indicate the direction of future work to overcome present limitations.

3.2. Thermodynamic Framework

Equilibrium between two phases L and V in a system containing m different components is described by m+2 equations:

$$T^L = T^V \tag{3-1}$$

$$P^L = P^V \tag{3-2}$$

$$\mu_i^L = \mu_i^V \text{ , for all } i \text{ .} \tag{3-3}$$

Nearly all existing equilibrium models for systems containing electrolytes use activity coefficients to calculate the chemical potential μ_i^L of the components in the liquid phase. A separate model, usually the ideal gas law, is used for the vapor phase.

At high pressures, or when supercritical components are present, equilibrium must be calculated from an equation of state. For most practical situations, the equation of state is an explicit function for pressure with temperature T, volume V, and the vector of mole numbers $\underline{n}_i$ as independent variables. When the Helmholtz energy A is expressed in terms of T, V, and $\underline{n}_i$, it is a thermodynamic potential. All quantities necessary for phase equilibrium calculations can be determined directly from A. The equation of state follows from

$$P = -\left(\frac{\partial A}{\partial V}\right)_{T,\underline{n}_i} = P\,(T, V, \underline{n}_i) \tag{3-4}$$

and the chemical potential μ_i is given by

$$\mu_i = \left(\frac{\partial A}{\partial n_i}\right)_{V,T,n_{j\neq i}} \tag{3-5}$$

μ_i can be written in terms of fugacity f_i:

$$\mu_i = \mu_i^0 + RT \ln \frac{f_i}{f_i^0} \tag{3-6}$$

Superscript ^{0} denotes the standard state, which is the pure ideal gas at temperature T and a pressure of 1 bar.

Substituting into equation (3-3), the condition for material equilibrium of component i becomes

$$f_i^L = f_i^V \tag{3-7}$$

or, using fugacity coefficients ϕ_i,

$$\phi_i^L x_i P = \phi_i^V y_i P \tag{3-8}$$

where x_i and y_i denote liquid and vapor phase mole fractions, respectively.

We write the Helmholtz energy as the sum of terms that result when the system is changed stepwise from pure ideal gases to the real mixture

$$A = \sum_{i=1}^{m} n_i a_i^0 + \Delta A_I + \Delta A_{II} + \Delta A_{III} + \Delta A_{IV} + \Delta A_V \tag{3-9}$$

where a_i^0 is the molar Helmholtz energy of pure species i in the standard state. ΔA_I denotes the change in free energy when the pure ideal gases are mixed at 1 bar and compressed to total volume V:

$$\Delta A_I = \sum_{i=1}^{m} n_i RT \ln \left(\frac{n_i RT}{P^0 V} \right) \tag{3-10}$$

R denotes the gas constant. The remaining terms in equation (3-9) are due to the interaction of particles in the mixture and to the charges of the ions.

The residual Helmholtz energy A^r is defined as the Helmholtz energy difference between the real system and a mixture of ideal gases at the same temperature T, volume V, and composition $\underline{n_i}$:

$$\begin{aligned} A^r &= A - \sum_{i=1}^{m} n_i a_i^0 - \Delta A_I \\ &= \Delta A_{II} + \Delta A_{III} + \Delta A_{IV} + \Delta A_V \end{aligned} \tag{3-11}$$

This work presents an expression for the residual Helmholtz energy of a mixture. The model is sufficiently general to include ionic components and volatile nonelectrolytes in addition to solvent molecules such as water.

We compute fugacity coefficients ϕ_i and pressure P from

$$\ln \phi_i = \left(\frac{\partial (A^r/RT)}{\partial n_i} \right)_{V,T,n_{j \neq i}} - \ln \left(\frac{PV}{nRT} \right) \tag{3-12}$$

and

$$P = - \left(\frac{\partial A^r}{\partial V} \right)_{T,\underline{n}_i} + \frac{nRT}{V} \tag{3-13}$$

where n is the total number of moles. The electrolyte species are considered to be completely dissociated into ions.

To calculate phase equilibria from an equation of state, equation (3-3) must be solved simultaneously for all components i. Topliss[2] developed a systematic procedure for this task. Extending his computer programs, we were able to include electrolyte components in the calculations. Appendix 1 gives a brief description of the necessary computations for phase equilibria. In Appendix 2, we describe the implementation of the equation of state into computer programs which interface with Topliss' procedure. This appendix also includes a listing of our routines.

3.3. An Equation of State for Nonelectrolyte Components

In a first step, we describe the uncharged molecules in the equilibrium mixture. We account for all contributions to the Helmholtz energy except those which result from the electric charges of the ions. We calculate the Helmholtz energy contributions of the intermolecular forces from a Lennard-Jones potential. Using perturbation theory, the potential is divided into two parts, a reference and a perturbation term.

The reference term accounts for the repulsive forces between the particles, the forces which determine the structure of the liquid. The steep repulsive portion of the Lennard-Jones potential is approximated by a hard sphere potential with diameter σ_i. Barker and Henderson[3] give a procedure for choosing the optimum σ_i as a function of temperature. We use the functional form given by Cotterman:[4]

$$\sigma_i = \sigma_i^* \frac{1 + 0.29770\,\tilde{T}}{1 + 0.33163\,\tilde{T} + 0.0010477\,\tilde{T}^2} \tag{3-14}$$

which accurately reproduces the results of Barker and Henderson's more complicated method. Here σ_i^* is the size parameter in the Lennard-Jones potential; it is an adjustable parameter for each pure component.

$\tilde{T}$ is a reduced temperature defined by

$$\tilde{T} = \frac{kT}{\varepsilon} \tag{3-15}$$

where k is Boltzmann's constant and ε is the Lennard-Jones energy parameter.

The Lennard-Jones potential in our model accounts for all attractive forces between uncharged molecules, including hydrogen bonding and multipole interactions. Therefore, we allow ε_i of each nonionic component to depend on temperature:

$$\frac{\varepsilon_i}{k} = \varepsilon_i^{(0)} + \varepsilon_i^{(1)} \exp\left(\varepsilon_i^{(2)} \frac{T}{T_{ci}}\right) \tag{3-16}$$

where T_{ci} is the critical temperature of component i and $\varepsilon_i^{(0)}$, $\varepsilon_i^{(1)}$, and $\varepsilon_i^{(2)}$ are adjustable parameters.

The Helmholtz energy for the reference mixture of hard spheres (relative to the mixture of ideal gases at the same temperature and density) is calculated from the Boublik-Mansoori[5,6] extension of the Carnahan-Starling equation

$$\Delta A_{II} = nRT \left[\frac{\frac{3DE}{F}\xi - \frac{E^3}{F^2}}{(1-\xi)} + \frac{\frac{E^3}{F^2}}{(1-\xi)^2} + \left(\frac{E^3}{F^2} - 1\right) \ln(1-\xi) \right] \tag{3-17}$$

$$D = \sum_{i=1}^{m} x_i \sigma_i \; ; \qquad E = \sum_{i=1}^{m} x_i \sigma_i^2 \; ; \qquad F = \sum_{i=1}^{m} x_i \sigma_i^3$$

$$\xi = \frac{\pi}{6} \rho N_{Av} F \; ; \qquad \rho = n/V$$

Here, $x_i = n_i/n$ is the mole fraction of species i, ρ is the molar density and N_{Av} is Avogadro's number.

The perturbation term gives the influence of attractive molecular forces. Barker and Henderson[3] showed that the contribution to the Helmholtz energy could be expressed as a series expansion in reciprocal temperature.

Truncating after the second term, we get

$$\Delta A_{III} = nRT \left(\frac{a^{(1)}}{\tilde{T}} + \frac{a^{(2)}}{\tilde{T}^2} \right) \tag{3-18}$$

$a^{(1)}$ and $a^{(2)}$ in equation (3-18) are functions of reduced molar density $\tilde{\rho}$, which is given by

$$\tilde{\rho} = \rho N_{Av} \sum_{i=1}^{m} x_i \sigma_i^3 \tag{3-19}$$

Barker and Henderson[7] used Monte Carlo computer simulation to evaluate $a^{(1)}$ and $a^{(2)}$ over a range of conditions. We express these functions as polynomials fitted to their results by Cotterman.[4]

$$a^{(1)} = -6.0782\,\tilde{\rho} - 2.2712\,\tilde{\rho}^2 - 0.75194\,\tilde{\rho}^3 + 2.5713\,\tilde{\rho}^4 \tag{3-20}$$

$$a^{(2)} = -1.3488\,\tilde{\rho} + 4.9862\,\tilde{\rho}^2 - 7.8545\,\tilde{\rho}^3 + 3.9760\,\tilde{\rho}^4 \tag{3-21}$$

The sum of contributions ΔA_{II} and ΔA_{III} provides a versatile equation of state for nonelectrolyte substances. To apply it towards equilibrium calculations, the parameters for each component must be known.

3.4. Evaluation of Parameters for Pure Components and Mixtures

For each nonelectrolyte component i, the four parameters σ_i^*, $\varepsilon_i^{(0)}$, $\varepsilon_i^{(1)}$, and $\varepsilon_i^{(2)}$ are adjusted to experimental data. Topliss developed computer programs which minimize the root-mean-square deviation between measured and calculated properties; his programs use a modified Levenberg-Marquardt algorithm from the MINPACK library of mathematical subroutines. For water, pure-component parameters are fit to vapor pressures and to vapor and liquid phase densities. Over the temperature range 0 to 320 °C, we represent the vapor pressures with a mean deviation of 0.6% and liquid densities with a mean deviation of 2.4%.

Because the critical temperature of CO_2 (31 °C) is near ambient conditions, we fitted the parameters for pure CO_2 to its critical properties as well as to its vapor pressure. This approach is vital to the representation of CO_2 solubility in aqueous mixtures in the temperature range of interest here. However, it sacrifices some accuracy in the calculation of liquid and supercritical densities of pure CO_2. Table 3-1 shows the pure-component parameters for H_2O and CO_2.

Table 3-1: Pure-Component Parameters for H_2O and for CO_2			
Parameter		H_2O	CO_2
σ_i^*	(10^{-8} cm)	3.0133	4.1254
$\varepsilon_i^{(0)}$	(K)	56.374	150.00
$\varepsilon_i^{(1)}$	(K)	640.93	177.28
$\varepsilon_i^{(2)}$	(–)	0.2925	0.9391
T_{ci}	(K)	647.35	304.20

For water, the energy parameter ε_i/k is in the range of 550 to 625 K and decreases with rising temperature, as is expected for a hydrogen-bonded fluid. The temperature dependence of ε_i for CO_2 is significant only at low temperatures; ε_i/k is close to 150 K for all the conditions relevant in this work.

To extend the equation of state to systems containing several components, a suitable method to calculate the Lennard-Jones parameter for the mixture, ε_{mix} is required. ε_{mix} is then used in equation (3-15) to determine the dimensionless temperature $\tilde{T}$. Following Van der Waals' one-fluid theory, we use a volume fraction mixing rule:

$$\varepsilon_{mix} = \frac{\sum_{i=1}^{m}\sum_{j=1}^{m} x_i x_j \sigma_{ij}^3 \varepsilon_{ij}}{\sum_{i=1}^{m} x_i \sigma_i^3} \qquad (3\text{-}22)$$

$$\sigma_{ij} = \frac{1}{2}(\sigma_i + \sigma_j)$$

σ_{ij} is the arithmetic average of the hard-sphere diameters of components i and j. The energy parameter ε_{ij} for the attraction between two unlike molecules is given by a corrected geometric-mean combining rule:

$$\varepsilon_{ij} = \sqrt{\varepsilon_i \, \varepsilon_j} \, (1 - k_{ij}) \tag{3-23}$$

$$k_{ij} = k_{ij}^{(1)} + \frac{k_{ij}^{(2)}}{T} \tag{3-24}$$

For the mixture H_2O / CO_2, the temperature-dependent k_{ij} is fitted to solubility data at various conditions obtained from the publications of Takenouchi and Kennedy[8] and Wiebe and Gaddy.[9, 10, 11] We obtain

$$k_{ij}^{(1)} = -0.0586 \; ; \quad k_{ij}^{(2)} = -69.51$$

The equation of state described above can be used to predict equilibrium properties of the binary mixture of H_2O and CO_2. Generally, this system is difficult to describe because the physical properties of the pure substances are markedly different. At room temperature, water is a hydrogen-bonded liquid whereas CO_2 is a volatile gas. Although CO_2 is itself a weak electrolyte, we neglect the formation of ions when it is dissolved in water. The molecular and ionic species of CO_2 in aqueous solution are not distinguished. This approach is justified because the dissociation constant is small.

We consider the variation with pressure of CO_2 solubility in aqueous solution . The points in Figure 3-1 represent experimental data at 150 °C, measured by Takenouchi and Kennedy.[8] In comparison, the continuous curve shows the prediction from our model. As the mole fraction of CO_2 approaches zero, the pressure must reduce to the vapor pressure of pure water at 45 °C (0.096 bar). Our model describes the shape of the solubility curve adequately, the deviations in the liquid phase mole fraction of CO_2 are less than 0.003 at all pressures below 100 MPa. Since only one temperature-dependent binary parameter was used for the mixture, this result is encouraging.

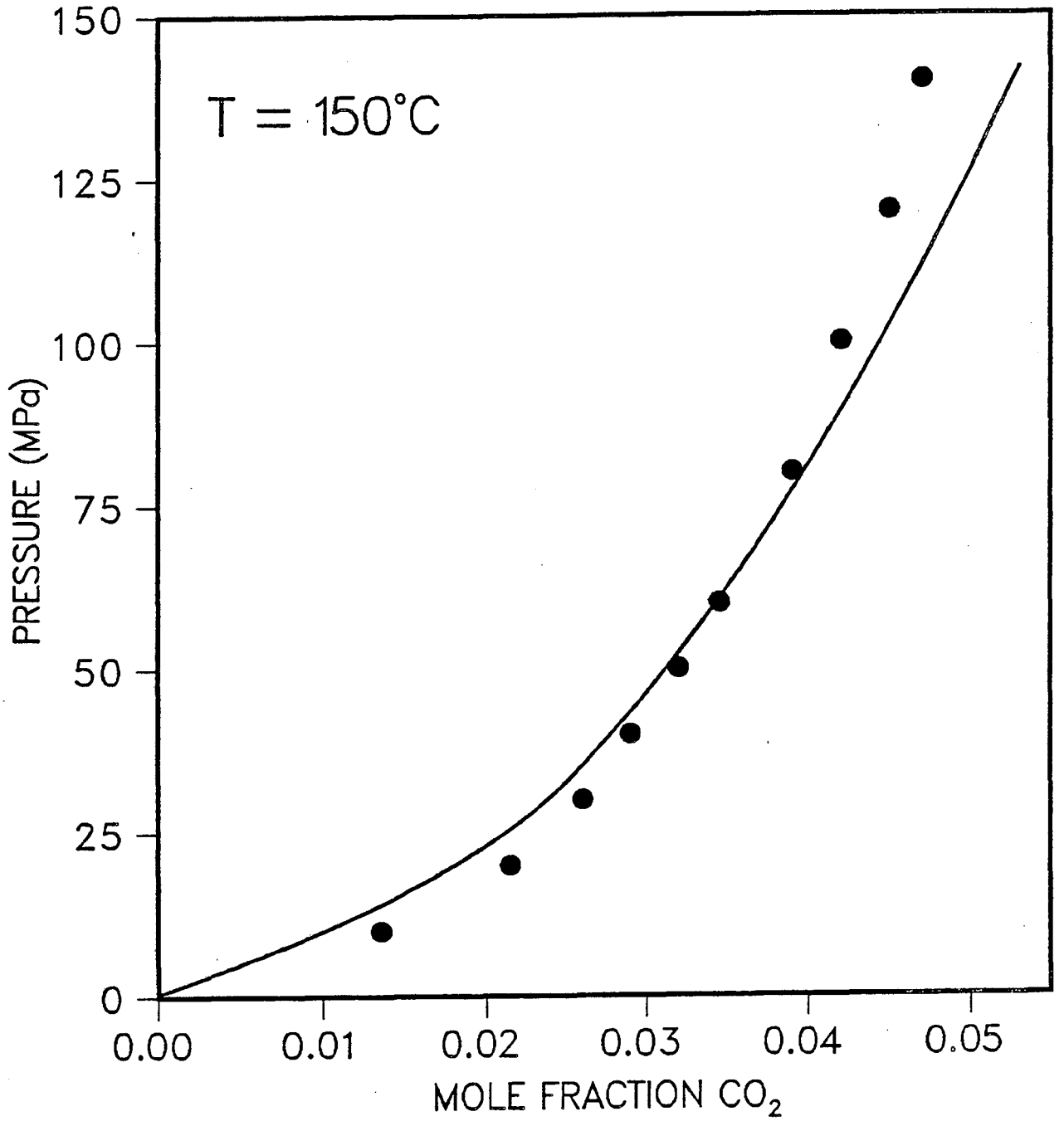

Figure 3-1: CO_2 Solubility in Water at 150°C

The next section discusses the effects of charged particles on the solution. Parameters σ_i^* and ε_i for the ions are required because the ions also contribute to the reference and perturbation terms ΔA_{II} and ΔA_{III}. We use values from crystal diffraction experiments[12] for the hard-sphere diameter σ_i^*. The Lennard-Jones parameter ε_i for ions is then calculated using dispersion theory:[13, 14]

$$\frac{\varepsilon_i}{k} = 2.2789 \times 10^{-8}\, \alpha_i^{1.5}\, Z_i^{1/2}\, (\sigma_i^*)^{-6} \qquad (3\text{-}25)$$

Here, Z_i is the number of electrons and α_i is the polarizability for an ion i. The numerical constant in equation (3-25) has units of (K cm$^{1.5}$).

Table 3-2 gives values of σ_i^*, ε_i, Z_i, and α_i for sodium and chloride ions.

Table 3-2: Parameters for Na^+ and Cl^- ions

Parameter		Na^+	Cl^-
σ_i^*	(10^{-8} cm)	1.90	3.62
$\varepsilon_i^{(0)}$	(K)	147.4	225.5
Z_i	(−)	10	18
α_i	(10^{-26} cm^3)	21.0	30.2

3.5. Contributions from Electrolyte Components

In this section, we examine the effect of assigning permanent electric charges to the ions in solution. This effect produces two important contributions to the Helmholtz energy of the mixture. The first describes the influence of ionic charges. The second reflects the electrostatic forces between the ions.

For the nonelectrolyte contributions to the equation of state, we used a discrete model of individual molecules for the fluid. Helmholtz energies ΔA_{II} and ΔA_{III} were calculated on a particle basis, directly expressing the interaction between two molecules. In principle, a similar picture could be used to describe ions in solution. Such a discrete-solvent model is shown schematically in the upper portion of Figure 3-2. However, at present we have no statistical-mechanical method for such systems which would give the analytic expressions for Helmholtz energy, as required for an equation of state.

Instead, we now regard the nonionic components in the mixture as a continuum. This assumption is called the primitive model, as pictured in the lower half of Figure 3-2. The influence of the solvent on the electrolyte contributions to the Helmholtz energy is expressed in the dielectric constant. We use a procedure developed by Harvey and Prausnitz[15] to calculate the dielectric constant of a mixture as a function of temperature, density, and composition.

ΔA_{IV} is the contribution to the Helmholtz energy that results from assigning a permanent charge to the ions in the solution. It reflects the interactions of the electrolytes with the bulk solvent phase, characterized by the dielectric constant D. For charging a sphere of diameter $\sigma_i^{(i)}$ in a continuum, an expression derived by Born[16] gives

$$\Delta A = \frac{N_{Av} e^2}{D} \sum_{i=1}^{m} \frac{n_i z_i^2}{\sigma_i^{(i)}} \tag{3-26}$$

Here, e is the unit charge of an electron, 1.602×10^{-19} Coulomb, and z_i is the charge number of ionic species i.

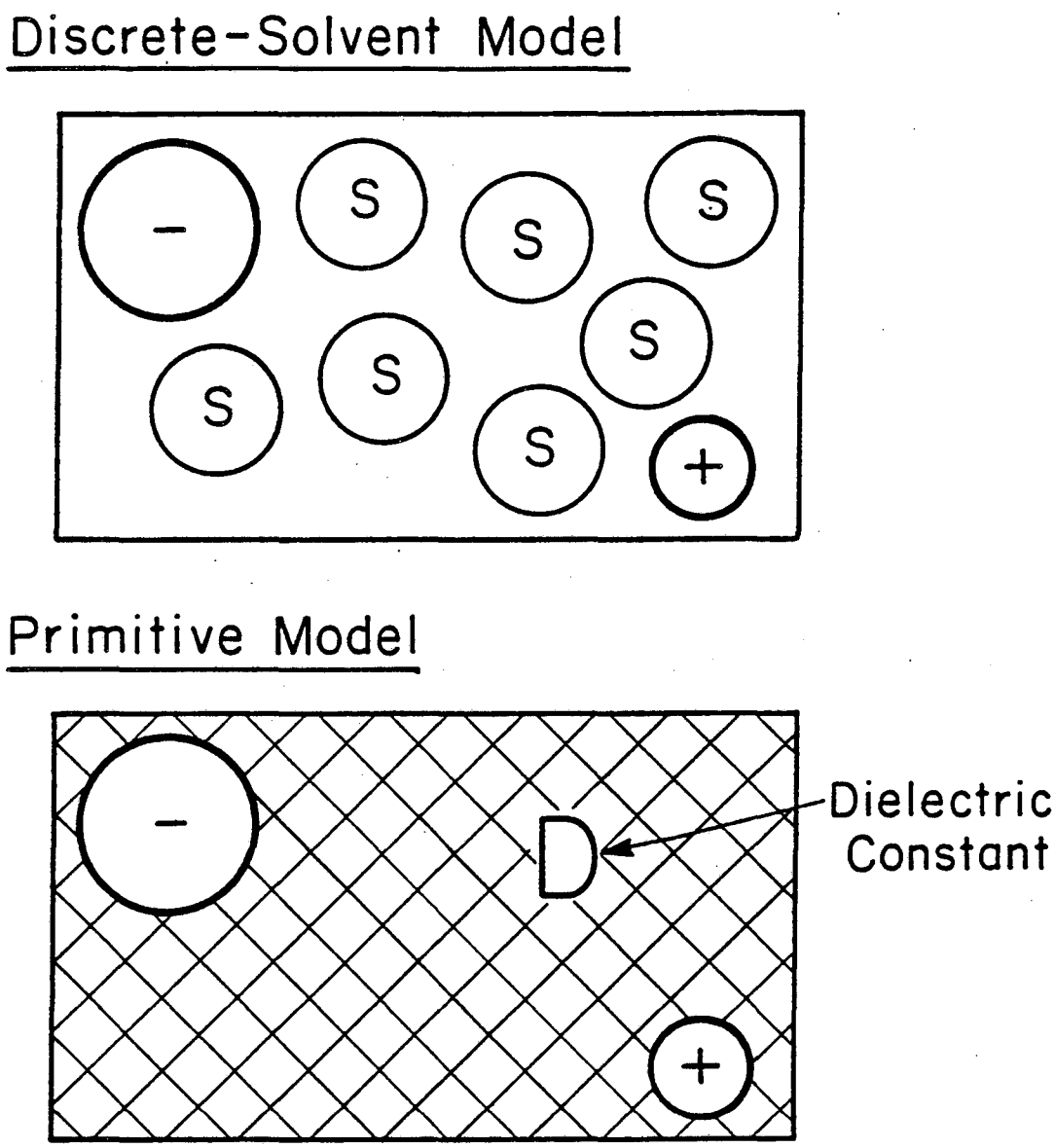

Figure 3-2: Models for Ionic Contributions

In our model, the ions are hard spheres of diameter $\sigma_i^{(i)}$ which occupy cavities of diameter $\sigma_i^{(c)}$ in the fluid. The dielectric constant of the cavity is that of a vacuum, $D_{Vacuum} = 1$. The bulk phase outside the cavity has the dielectric constant D of the continuous solution. From Born's expression, we obtain

$$\Delta A = N_{Av} e^2 \sum_{i=1}^{m} n_i z_i^2 \left(\frac{1}{D\sigma_i^{(c)}} + \frac{1}{\sigma_i^{(i)}} - \frac{1}{\sigma_i^{(c)}} \right) \quad . \tag{3-27}$$

We use the crystal-diffraction results for $\sigma_i^{(i)}$ of the ions. Rashin and Honig[17] give values for the cavity diameter $\sigma_i^{(c)}$. They argue that $\sigma_i^{(c)}$ for anions is essentially the same as the crystal diameter $\sigma_i^{(i)}$, while for cations, the cavity is larger than the particle, due to the orientation of water molecules around a positive charge. Table 3-3 shows the diameters used for the calculation of the Helmholtz energy that results from charging Na^+ and Cl^- ions.

Table 3-3: Crystal and Cavity Diameters for Na^+ and Cl^- ions

Diameter, 10^{-8} cm	Na^+	Cl^-
$\sigma_i^{(i)}$	1.90	3.62
$\sigma_i^{(c)}$	3.14	3.62

The electrostatic forces between ions in the mixture give rise to the term ΔA_V for Helmholtz energy. In their well-known model, Debye and Hückel[18] describe the interactions between a central ion and a surrounding charge cloud. Pitzer[19,20] extended this approach in a virial expansion of electrolyte concentration. He obtained good results for solutions in pure solvents up to moderate molalities by adjusting parameters to experimental data.

To apply this method to systems containing more than one solvent, parameters for the salt in each of the pure solvents must be fitted. The parameters in the mixed-solvent system must then be calculated from

arbitrary mixing rules. This approach was used by Raatschen[21] to describe the ternary system water/methanol/LiBr.

If considerable amounts of a supercritical gas are dissolved in an aqueous phase, the above method fails because no data exist for the salt in the pure supercritical component. Mixtures like $H_2O/NaCl/CO_2$ at high pressures must be treated by a different approach.

The Mean Spherical Approximation (MSA) is used for the equation of state in this work. This theoretical model has been solved for systems containing electrolytes of different sizes by Blum.[22] However, his expressions for the thermodynamic properties are too complicated to use in an equation of state. Instead, we use a simplified model which treats all ions as spheres of equal size with a mean ionic diameter, as given by Waisman and Lebowitz.[23] The influence of the solvent is determined only from the dielectric constant; no data for the salt in the pure solvents are required. The corresponding expression for the Helmholtz energy resulting from ion-ion interactions is

$$\Delta A_V = -\frac{(2\Gamma)^3 (1 + 1.5\,\Gamma\sigma_i^{(m)})}{12\pi N_{Av}\rho} \quad . \tag{3-28}$$

Γ is called the screening length, it is given by

$$\Gamma = \frac{1}{2\,\sigma_i^{(m)}} \left(\sqrt{1 + 2\sigma_i^{(m)}\kappa} - 1 \right) \tag{3-29}$$

$$\kappa^2 = \frac{4\pi e^2 N_{Av}\rho}{DkT} \sum_{i=1}^{m} x_i z_i^2$$

In equations (3-28) and (3-29), $\sigma_i^{(m)}$ is the mean ionic diameter, calculated by averaging only over the mole fraction of ions. If p ionic species are present in the solution,

$$\sigma_i^{(m)} = \frac{\sum_{i=1}^{p} x_i \sigma_i^{(i)}}{\sum_{i=1}^{p} x_i} \tag{3-30}$$

Again, we use the values given in Table 3-3 for diameter $\sigma_i^{(i)}$ of the ions.

3.6. Results for Solutions of Electrolytes

The equation of state containing Helmholtz energy terms ΔA_{II} to ΔA_V is useful in predicting vapor-liquid equilibria for electrolyte solutions. We examine first results for the binary system H_2O / NaCl, and second for the ternary mixture H_2O / NaCl / CO_2.

Vapor-liquid equilibria in salt solutions are conveniently described in terms of the osmotic coefficient Ω. For a 1:1 electrolyte, it is given by

$$\Omega = -\frac{1}{2mW_s} \ln \frac{P_s}{P_s^0} \tag{3-31}$$

Subscript s indicates the solvent, W_s is its molecular weight. The concentration of electrolytes is given in terms of molality m (moles salt / kg solvent) of the undissociated salt. The vapor pressure of the solution P_s is smaller than the vapor presure P_s^0 of the pure solvent at the same temperature. At infinite dilution, the osmotic coefficient approaches unity.

Figure 3-3 shows experimental and predicted results for aqueous solutions of sodium chloride. The dotted line drawn through data points from the compilation of Hamer and Wu[24] exhibits a minimum at low molalities and a steady increase with higher concentrations. The predicted osmotic coefficients from our model are plotted in the dashed line; they show the correct behavior at very low concentrations. At higher molalities, the calculated values are clearly too small, indicating positive deviations of the calculated vapor pressure from the measured data.

An additional investigation showed, however, that a model using only the Debye-Hückel theory for ion-ion interactions gives even lower values for the osmotic coefficients. The extension due to Pitzer[19] improves the results of the Debye-Hückel theory somewhat; however, the osmotic coefficients obtained from the Mean Spherical Approximation come closest to the experimental data. The shape of the curves obtained from the simple and extended Debye-Hückel theories is similar to the plot for the Mean Spherical Approximation.

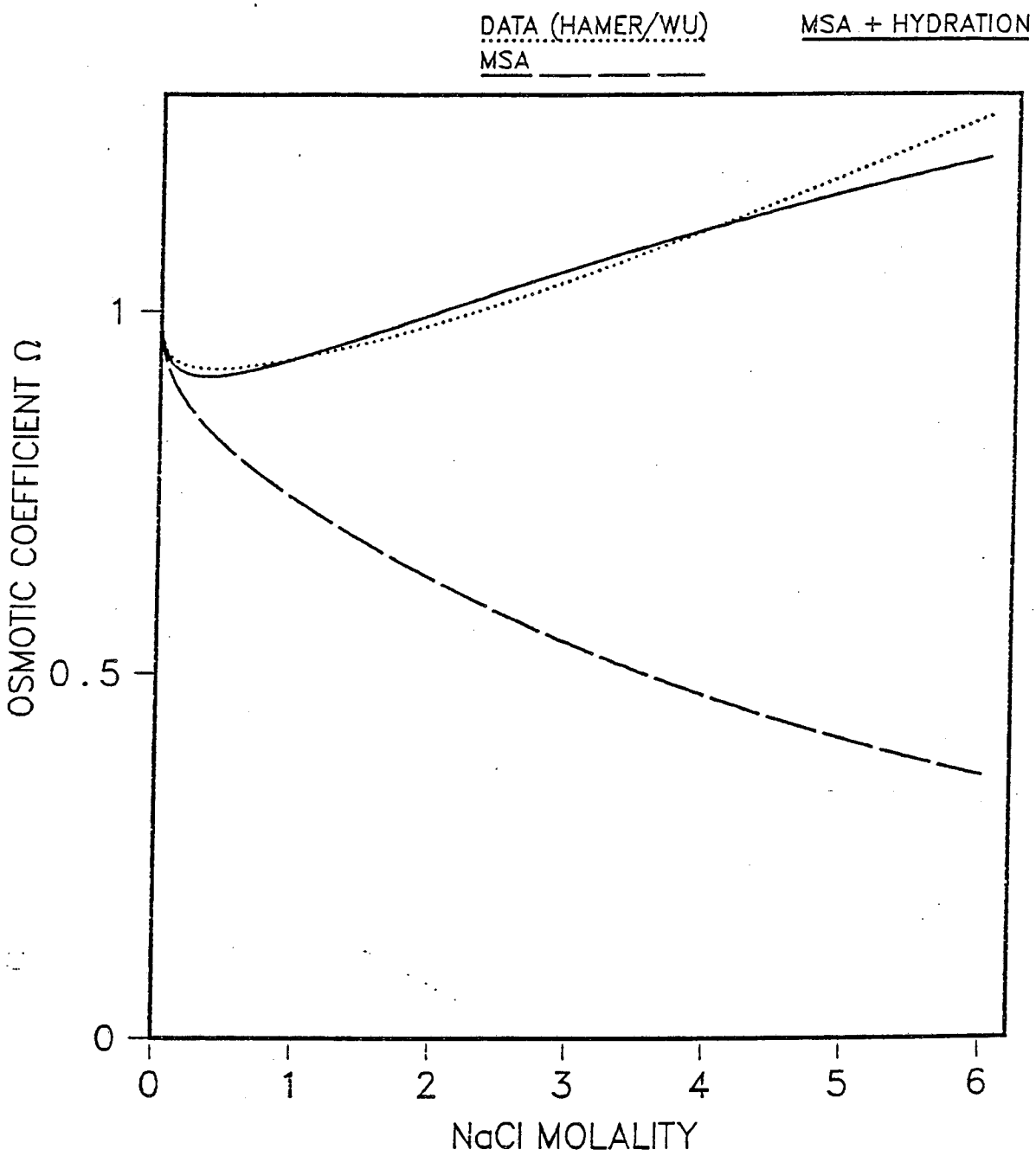

Figure 3-3: Osmotic-Coefficient Prediction for NaCl / Water at 25°C

Apparently, our model does not account for all attractive intermolecular forces that prevail in the solution. Due to the limitations of the primitive model, we have not included short-range ion-solvent interactions such as hydration. In the direct vicinity of an ion, the polar water molecules are oriented by the permanent charge. For example, a positive cation attracts the more negative oxygen atom of the water molecule. These orientation effects probably lower the fugacity of the water in all but extremely dilute solutions, resulting in a lower vapor pressure for the mixture.

To test this hypothesis, we simulated hydration effects by adjusting a binary parameter k_{ij} from equation (3-23) for the water-salt pairing. Although hydration is not a Lennard-Jones type interaction, this method results in effective attraction between the salt and the solvent. Using the same value for both the H_2O / Na^+ and the H_2O / Cl^- pairs, the experimental data was best represented with a $k_{ij} = -0.35$.

The continuous line in Figure 3-3 shows the predicted osmotic coefficients when hydration is taken into account. This line is much closer to the experimental values than the previous result, indicating a deficiency of the primitive model. Short-range interactions between the ions and the surrounding water molecules appear to play an important role for phase equilibria of aqueous solutions; they cannot be neglected in model calculations.

When electrolytes are added to a binary solvent, the liquid phase concentration of the solvent with the lower dielectric constant usually decreases while its vapor phase concentration increases. This is the well-known salting-out effect. The liquid mixture effectively increases its dielectric constant, thereby lowering the Helmholtz energy of the charge of the ions and of the ion-ion interactions. This effect has been shown experimentally for many systems of electrolytes in mixed solvents.

At low pressures, the solubility of nonpolar gases in aqueous solutions follows Henry's law. The fugacity of the dissolved gas in the liquid phase is given by

$$f_i^L = H_i \, x_i \tag{3-32}$$

where x_i is the mole fraction of dissolved gas. We let H_i^0 denote the Henry's

constant for the gas dissolved in pure water.

When a dissolved gas is salted out of solution, its Henry's constant H_i increases. The empirical Setchenow equation relates the change in Henry's constant to the concentration of salt in solution.

$$\log\left(\frac{H_i}{H_i^0}\right) = k_s m \tag{3-33}$$

The concentration is usually given in terms of molality (moles salt / kg solvent); k_s is the empirical Setchenow coefficient, its units are inverse concentration. While k_s is strictly defined as $m \rightarrow 0$, the same value will often fit data up to moderate salt concentrations. Long and McDevit[25] evaluated experimental solubility data at 25°C to obtain a k_s of 0.101 $(\text{mol/kg})^{-1}$ for CO_2 in NaCl solutions.

The equation of state presented in this work is used to determine Henry's constants for CO_2 in pure water and in dilute NaCl solutions. The model gives a Setchenow coefficient of 0.115 $(\text{mol/kg})^{-1}$ at 25°C, which is in good agreement with the experimental value.

Next, we predict the effect of salt on the solubility of CO_2 in water up to high pressures. If we do not account for hydration ($k_{ij} = 0$ for H_2O / salt interactions), the calculated curve in Figure 3-1 is shifted slightly toward higher CO_2 mole fractions when salt is added. This is contrary to experimental findings, again indicating that the primitive model neglects important contributions to the Helmholtz energy of the mixture.

The calculations were repeated using the binary parameter obtained earlier ($k_{ij} = -0.35$) to simulate hydration of the salt. The solid line in Figure 3-4 again shows the solubility of CO_2 in pure water at 150°C; the open points are experimental data for 6 and 20 weight percent salt solutions, measured by Takenouchi and Kennedy.[26] Similar results are calculated at 200 and 250°C.

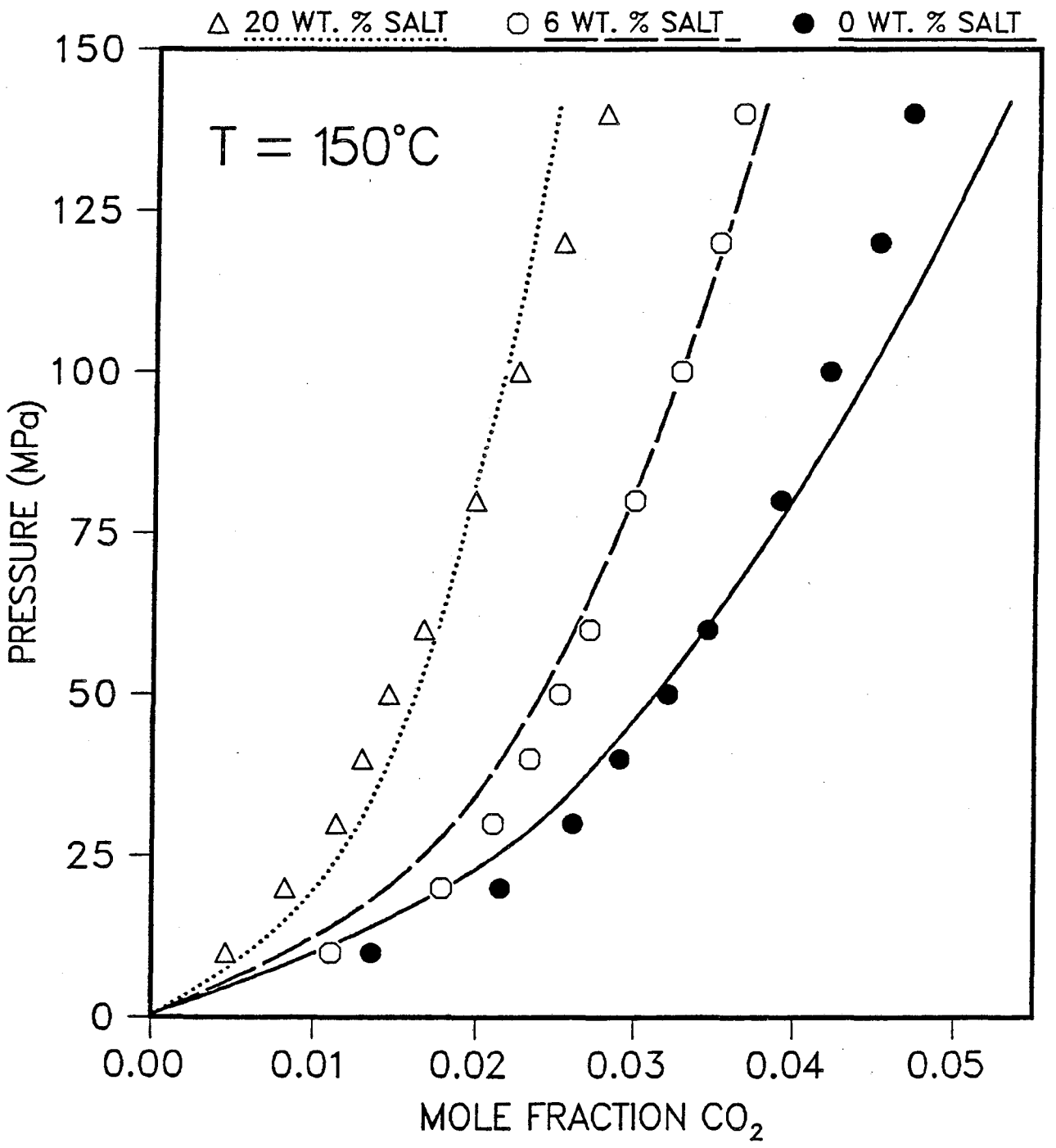

Figure 3-4: CO_2 Solubility in Water and NaCl Solutions at 150°C

The solubility of CO_2 decreases drastically when ions are introduced into the solution. Including the hydration term, our equation of state gives the dashed and the dotted lines for solutions of the given concentrations. The curves are correctly shifted to lower CO_2 mole fractions in the liquid phase as salt is added, indicating the salting-out effect. At pressures up to approximately 100 MPa, we predict the change in CO_2 solubility well when 6 weight percent salt is added to the system. For the solution of 20 weight percent salt, the calculated decrease in CO_2 mole fraction is somewhat smaller than the experimental values. As the solution becomes more concentrated in salt, further interactions which our equation of state does not take into account may become important. For example, at higher salt concentrations, the charged particles in the solution may influence the forces between the water and CO_2 molecules. These are in effect three-body interactions which cannot be described with an equation of state using only binary parameters. Also, the curve of predicted osmotic coefficients showed deviations at higher salt concentrations; ion-solvent interactions are not represented adequately in this region.

At the highest pressures shown in Figure 3-4, our model predicts too much salting-out; the calculated decrease in CO_2 solubility is larger than indicated by the experiments. As the correction for hydration presented here is only preliminary, this result is not surprising. The high pressures are likely to influence the short-range interactions between ions and solvent molecules; such effects cannot be described by modelling hydration as a Lennard-Jones type interaction.

4. Conclusions

This work contributes to both the experimental and the theoretical studies of phase equilibrium thermodynamics for mixtures containing aqueous electrolytes and volatile components.

An apparatus was designed and constructed to measure reliable composition data for both vapor and liquid equilibrium phases. It can be used for mixtures of aqueous electrolytes and nonelectrolytes from ambient to 250°C and 140 MPa. The components in the equilibrium chamber are mixed by a circulation system. Small samples from both phases can be drawn through capillary lines and analyzed in a gas chromatograph. The salt concentration is measured when initially charging the mixture into the equilibrium cell.

Experimental safety is crucial to high-pressure equipment, especially if combustible gases are present. A prime factor in the design of the apparatus is secure control over potential dangers.

Molecular-thermodynamic models for vapor-liquid equilibria are based on results from statistical mechanics. In this work, an equation of state is developed for calculation of equilibria in mixtures of aqueous electrolytes and nonelectrolytes over a wide range of conditions. Based on an expression for the Helmholtz energy, it is applicable to all practical fluid densities. A simple correction is used to overcome deficiencies in the primitive model. Using only binary data, we successfully describe salting-out behavior at pressures up to 100 MPa for the ternary system H_2O / NaCl / CO_2.

Acknowledgement

This work was supported by the Director, Office of Energy Research, Office of Basic Energy Sciences, Chemical Sciences Division of the U.S. Department of Energy under Contract No. DE-AC03-76SF00098.

References

1. D.H.Ziger and C.A. Eckert, "Simple High-Pressure Magnetic Pump," *Rev. Sci. Instrum.*, vol. 53, p. 1296, 1982.

2. R. Topliss, "Techniques to Facilitate the Use of Equations of State for Complex Fluid-Phase Equilibria," Ph.D. Thesis, University of California, Berkeley, 1985.

3. J.A. Barker and D. Henderson, "Perturbation Theory and Equation of State for Fluids. II. A Successful Theory of Liquids," *J. Chem Phys.*, vol. 47, p. 4714, 1967.

4. R. Cotterman, "Phase Equilibria for Complex Fluid Mixtures at High Pressure," Ph.D. Thesis, University of California, Berkeley, 1985.

5. T. Boublik, "Hard-Sphere Equation of State," *J. Chem. Phys.*, vol. 53, pp. 471-472, 1970.

6. G.A. Mansoori, N.F. Carnahan, K.E. Starling, and T.W. Leland, "Equilibrium Thermodynamic Properties of the Mixture of Hard Spheres,," *J. Chem. Phys.*, vol. 54, pp. 1523-1525, 1971.

7. D. Henderson and J.A. Barker, "Perturbation Theories," in *Physical Chemistry, An Advanced Treatise*, ed. by H. Eyring, D. Henderson, W. Jost, vol. 8a, Academic Press, New York, 1971.

8. S. Takenouchi and G. C. Kennedy, "The Binary System H_2O–CO_2 at High Temperatures and Pressures," *Am. Jour. Sci.*, vol. 262, pp. 1055-1074, 1964.

9. R. Wiebe and V.L. Gaddy, "The Solubility in Water of Carbon Dioxide at 50, 75 and 100°, at Pressures to 700 Atmospheres," *J. Am. Chem. Soc.*, vol. 61, pp. 315-318, 1939.

10. R. Wiebe and V.L. Gaddy, "The Solubility of Carbon Dioxide in Water at Various Temperatures from 12 to 40° and at Pressures to 500 Atmospheres. Critical Phenomena," *J. Am. Chem. Soc.*, vol. 62, pp. 815-817, 1940.

11. R. Wiebe and V.L. Gaddy, "Vapor Phase Composition of Carbon-Dioxide Water Mixtures at Various Temperatures and at Pressures to 700 Atmospheres," *J. Am. Chem. Soc.*, vol. 63, pp. 475-477, 1941.

12. J.A. Dean, ed., *Lange's Handbook of Chemistry,* McGraw-Hill, New York, 1985.

13. C. Mavroyannis and M.J. Stephen, "Dispersion Forces," *Mol. Phys.*, vol. 5, pp. 629-638, 1962.

14. W.L. Masterson and T.P. Lee, "Salting Coefficients from Scaled Particle Theory," *Phys. Chem.*, vol. 74, pp. 1776-1782, 1970.

15. A.H. Harvey and J.M. Prausnitz, "Dielectric Constants of Fluid Mixtures over a Wide Range of Temperature and Density," Journal of Solution Chem., in press, 1987.

16. M. Born, "Volumen und Hydrationswärme der Ionen," *Zeitschrift für Physik*, vol. 1, pp. 45-48, 1920.

17. A. Rashin and B. Honig, "Reevaluation of the Born Model for Ion Hydration," *J. Phys. Chem.*, vol. 89, pp. 5588-5593, 1985.

18. P. Debye and E. Hückel, "Zur Theorie der Elektrolyte," *Phys. Zeitschrift*, vol. 24, pp. 185-206, 1923.

19. K.S. Pitzer, "Thermodynamics of Electrolytes. I. Theoretical Basis and General Equations," *J. Phys. Chem.*, vol. 77, pp. 268-277, 1973.

20. K.S. Pitzer and J.J. Kim, "Thermodynamics of Electrolytes. IV. Activity and Osmotic Coefficients for Mixed Electrolytes," *J. Amer. Chem. Soc.*, vol. 96, pp. 5701-5707, 1974.

21. W. Raatschen, A.H. Harvey, and J.M. Prausnitz, "Equation of State for Solutions of Electrolytes in Mixed Solvents," Fluid Phase Equilibria, in press, 1987.

22. L. Blum, "Primitive Electrolytes in the Mean Spherical Approximation," in *Theoretical Chemistry: Advances and Perspectives*, vol. 5, pp. 1-66, Academic Press, New York, 1980.

23. E. Waisman and J.L. Lebowitz, "Mean Spherical Model Integral Equation for Charged Hard Spheres I. Method of Solution," *J. Chem. Phys.*, vol. 56, pp. 3086-3099, 1972.

24. W.J. Hamer and Y.C. Wu, *J. Phys. Chem. Ref. Data*, vol. 1, pp. 1047-1100., 1972.

25. F. A. Long and W. F. McDevit, "Activity Coefficients of Nonelectrolyte Solutes in Aqeous Salt Solutions," *Chem. Rev.*, vol. 38, pp. 119-169, 1951.

26. S. Takenouchi and G. C. Kennedy, "The Solubility of Carbon Dioxide in NaCl Solutions at High Temperatures and Pressures," *Am. Jour. Sci.*, vol. 263, pp. 445-454, 1965.

5. NOMENCLATURE

A	Helmholtz energy
D	dielectric constant
D,E,F	defined in Equation (3-17)
H	Henry's constant
N_{Av}	Avogadro's number
P	pressure
R	gas constant
T	temperature
V	total volume
W	molecular weight
Z	number of electrons on ion
a	molar Helmholtz energy
a	functions in Equation (3-18)
e	unit electronic charge
f	fugacity
k	Boltzmann's constant
k_{ij}	adjustable binary parameter in Equation (3-23)
k_s	Setchenow coefficient
m	molality
m	number of components
n	number of moles
p	number of ionic species
v	molar volume
x	mole fraction in liquid phase
y	mole fraction in vapor phase
z	mole fraction in either phase
z	charge number

Greek Letters:

α	polarizability
β_i	parameter in Equation (A2-4)
ε	energy parameter in Lennard-Jones potential
κ	defined after Equation (3-29)
μ	chemical potential
ϕ	fugacity coefficient
ρ	molar density
$\sigma_i^{(c)}$	cavity diameter
$\sigma_i^{(i)}$	ionic diameter
$\sigma_i^{(m)}$	mean ionic diameter
σ	temperature-dependent hard-sphere diameter
σ^*	adjustable Lennard-Jones distance parameter
ξ	reduced density parameter in Equation (3-17)
Γ	screening length
Ω	osmotic coefficient

Superscripts:

L	liquid phase
V	vapor phase
r	residual
0	standard state
0	quantity in pure solvent
(0),(1),(2)	number of adjustable parameter
~	reduced quantity (used on temperature and density)

Subscripts:

i,j	component i or j
ij	interaction between molecules i and j
s	solvent
I...V	contributions to A^r
$\underline{o}$	vector quantity

Appendix 1: Phase-Equilibrium Calculations from an Equation of State

The number of degrees of freedom f in a system containing m components in p phases is given by Gibbs's phase rule:

$$f = m - p + 2 \tag{A1-1}$$

If f conditions are specified, the remaining thermodynamic quantities which describe the phase equilibrium can be determined from an equation of state (EOS).

As an example, we consider a vapor-pressure calculation for a mixture of m components. Temperature T and $m-1$ liquid phase concentrations x_i are fixed, x_m follows because the sum of mole fractions must add up to unity for each phase. We have to solve for $m+2$ unknowns, the pressure P, $m-1$ vapor phase concentrations, and the molar densities of both phases, ρ^V and ρ^L. For this equilibrium problem, $m+2$ independent equations must be satisfied simultaneously. For each of the m components, we have

$$f_i^L = f_i^V \ , \tag{A1-2}$$

where the fugacities f_i^L and f_i^V are found from the EOS. The remaining two constraints result from the determination of vapor and liquid densities from the EOS.

In practice, equilibrium calculations follow an iterative procedure. For the vapor-pressure problem, we start from initial guesses for pressure P and the vector of vapor mole fraction $\underline{y_i}$. Next, the EOS is solved for the densities of both phases. As density is an independent variable in the EOS, a trial-and-error solution must be used for this step. When the values of T, ρ, and composition $\underline{z_i}$ are fixed for each phase, fugacity coefficients ϕ_i^L and ϕ_i^V can be calculated.

The condition for material equilibrium as given by equation (3-6) is written as

$$y_i = \frac{\phi_i^L}{\phi_i^V} x_i \ , \tag{A1-3}$$

providing a new estimate for the vapor-phase composition. The above calculations for ρ and ϕ_i are repeated until the iteration converges on a vector of mole fractions $\underline{y'}_i$. However, unless the initial guess for the vapor pressure P was correct, the sum of $\underline{y'}_i$ will not be equal to unity, as required. The algorithm chooses a new value for P and the iteration for the vapor-phase composition is entered again. When the sum of calculated $\underline{y'}_i$ converges to unity, the equilibrium problem is solved and the desired values for P, ρ^V, ρ^L, and $\underline{y}_i$ are determined.

The computational effort for determining phase equilibria from an equation of state is large. In a typical calculation as illustrated above, the EOS is evaluated for pressure well over 100 times. Computational efficiency is very important when implementing an EOS into computer programs. In Appendix 2, we outline the procedure used in this work, which was suggested by Topliss.

Appendix 2: Implementation of the Equation of State into Computer Programs

The equations given in section 3.2 use an equation of state (EOS) of the form

$$P = P(T, V, \underline{n}_i) \tag{A2-1}$$

where $\underline{n}_i$ is the vector of mole numbers. For computational purposes, the function

$$P = P(T, \rho, \underline{z}_i) \tag{A2-2}$$

is much more convenient. The two are directly related; the density ρ is given by $\rho = V / n$ and the mole fraction z_i is defined as $z_i = n_i / n$, where n is the total number of moles.

Accordingly, our implementation uses an expression for the Helmholtz energy of the form

$$A = A(T, \rho, \underline{z}_i) \tag{A2-3}$$

to evaluate the pressure and the fugacity coefficients.

By including the partial derivatives of the fugacity coefficients with respect to temperature, pressure, and composition, the efficiency of calculating phase equilibria can be greatly increased. Also, in the critical and retrograde regions, the computation does not easily converge without these derivatives.

Partial derivatives can be calculated numerically using finite-difference approximations. However, an analytical method where explicit expressions for the derivatives are evaluated is often more precise. If a systematic procedure is used, the computational effort of finding the partial derivatives of the fugacity coefficients with respect to composition analytically from an EOS is not exceedingly large.

In his dissertation, Topliss suggests parameterization of the EOS for computational efficiency. To use his model for phase equilibrium calculations and for fitting adjustable parameters to experimental data, an EOS must be written as

$$A = A\,(T,\rho,\underline{\beta}_i) \qquad \text{(A2-4)}$$

$\underline{\beta}_i$ is a vector of composition-dependent parameters which can be chosen arbitrarily for a particular EOS. These parameters may also depend on density or temperature, as is often necessary for complicated equations of state. However, the computation is most efficient if the β_i are functions only of composition.

The computer programs of the EOS evaluate the expressions for the parameters β_i and calculate the function $A = A(T,\rho,\underline{\beta}_i)$. In addition, the necessary partial derivatives of A and of $\underline{\beta}_i$ are implemented as explicit functions. The routines from Topliss' procedure use these values to solve a given equilibrium problem.

The curves for solubility of CO_2 in water and aqueous salt solutions were generated with the aid of a multicomponent flash routine written originally by Topliss and modified to work with systems containing salt.

Due to the iterative nature of finding the density ρ from an EOS when the pressure P, temperature T, and composition $\underline{z}_i$ are specified, the EOS is often evaluated repeatedly for the same values of T and $\underline{z}_i$, but at different values of ρ. Therefore, the EOS is best implemented as two separate routines, the first of which determines only those expressions that do not depend on density. Then it calls the second routine, which calculates the density-dependent terms. A density-finding algorithm can evaluate the second routine repeatedly without repeating unnecessary calculations. Once the algorithm has converged on a value for the desired density, the first routine is called again with a different control flag. This time it calculates the terms necessary to find the fugacity coefficients and their respective partial derivatives at the specified density, as required for phase-equilibrium calculations.

In addition to the two routines described above, our implementation includes two more subroutines which are used to initialize EOS-specific quantities before a calculation. The following are brief descriptions of our routines; the listings of the programs are available upon request.

EOSRD

This routine reads pure-component and binary parameters from an INPUT data file, stores them in corresponding variables and writes the on an OUTPUT file for reference. The routine needs to be executed only once for each application of the EOS to a particular system.

EOSINT

This routine stores pure-component and binary parameters in appropriate COMMON-blocks for the main EOS-routines. It is executed only once in normal applications, however, when the EOS is used to adjust parameters to experimental data, this initialization routine is called for each new set of parameters.

EOS

The main EOS-routine serves two purposes. In its upper portion, it evaluates all terms for the EOS which are necessary to calculate the pressure, but which do not depend on density ρ. This is in preparation for the call to routine PRES. In its lower part, EOS evaluates all expressions necessary to calculate the fugacity coefficients and their partial derivatives for a given density ρ.

PRES

The routine PRES calculates the pressure of a pure component or mixture at specified conditions of $(T, \rho, \underline{z}_i)$. PRES is the routine which is called most frequently in equilibrium calculations from the EOS.

LAWRENCE BERKELEY LABORATORY
TECHNICAL INFORMATION DEPARTMENT
UNIVERSITY OF CALIFORNIA
BERKELEY, CALIFORNIA 94720